Mapping brain circuitry with a light microscope

Pavel Osten[1] & Troy W Margrie[2,3]

The beginning of the 21st century has seen a renaissance in light microscopy and anatomical tract tracing that together are rapidly advancing our understanding of the form and function of neuronal circuits. The introduction of instruments for automated imaging of whole mouse brains, new cell type–specific and trans-synaptic tracers, and computational methods for handling the whole-brain data sets has opened the door to neuroanatomical studies at an unprecedented scale. We present an overview of the present state and future opportunities in charting long-range and local connectivity in the entire mouse brain and in linking brain circuits to function.

Since the pioneering work of Camillo Golgi and Santiago Ramón y Cajal at the turn of the last century[1,2], advances in light microscopy (LM) and neurotracing methods have been central to the progress in our understanding of anatomical organization in the mammalian brain. The Golgi silver-impregnation method allowed the visualization of neuron morphology, providing the first evidence for cell type–based and connectivity-based organization in the brain. The introduction of efficient neuroanatomical tracers in the second half of the last century greatly increased the throughput and versatility of neuronal projection mapping, which led to the identification of many anatomical pathways and circuits, and revealed the basic principles of hierarchical and laminar connectivity in sensory, motor and other brain systems[3,4].

The beginning of this century has seen a methods-driven renaissance in neuroanatomy, one that is distinguished by a focus on large-scale projects that yield unprecedented amounts of anatomical data. Instead of the traditional 'cottage-industry' approach to studying one anatomical pathway at a time, the new projects aim to generate complete data sets—so-called projectomes and connectomes—that can be used by the scientific community as resources for answering specific experimental questions. These efforts range in scale and resolution from the macroscopic to the microscopic: from studies of the human brain by magnetic resonance imaging to reconstructions of dense neural circuits in small volumes of brain tissue by electron microscopy (see Review[5] and Perspective[6] in this Focus).

Advancements in LM methods, the focus of this Review, are being applied to the mapping of point-to-point connectivity between all anatomical regions in the mouse brain by means of sparse reconstructions of anterograde and retrograde tracers[7]. Taking advantage of the automation of LM instruments, powerful data-processing pipelines, and combinations of traditional and modern viral vector-based tracers, teams of scientists at Cold Spring Harbor Laboratory (CSHL), Allen Institute for Brain Science (AIBS) and University of California Los Angeles (UCLA) are racing to complete a connectivity map of the mouse brain—dubbed the 'mesoscopic connectome'—which will provide the scientific community with online atlases for viewing entire anatomical data sets[7]. These efforts demonstrate the transformative nature of today's LM-based neuroanatomy studies and the astonishing speed with which large amounts of data can be disseminated online, and have an immediate impact on research in neuroscience laboratories around the world.

As the mouse mesoscopic connectomes are being completed, it is clear that LM methods will continue to impact the evolution of biological research and specifically neuroscience: new trans-synaptic viral tracers are being engineered to circumvent the need to resolve synapses, which has constrained the interpretation of cell-to-cell connectivity in LM studies, and new assays

[1]Cold Spring Harbor Laboratory, Cold Spring Harbor, New York, USA. [2]Department of Neuroscience, Physiology and Pharmacology, University College London, London, UK. [3]Division of Neurophysiology, The Medical Research Council National Institute for Medical Research, London, UK. Correspondence should be addressed to P.O. (osten@cshl.edu) or T.W.M. (tmargri@nimr.mrc.ac.uk).

RECEIVED 2 MARCH; ACCEPTED 15 APRIL; PUBLISHED ONLINE 30 MAY 2013; DOI:10.1038/NMETH.2477

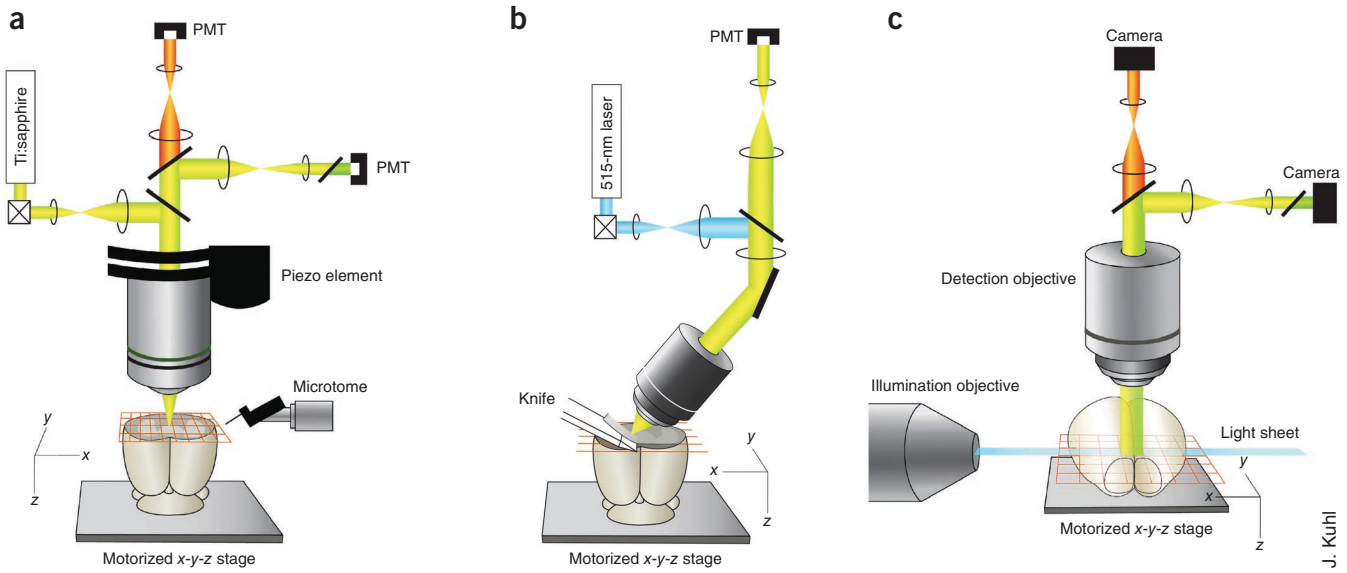

Figure 1 | Whole-brain LM methods. (**a**) In STP tomography, a two-photon microscope is used to image the mouse brain in a coronal plane in a mosaic grid pattern, and a microtome sections off the imaged tissue. Piezo objective scanner can be used for *z*-stack imaging (image adapted from ref. 15). (**b**) In fMOST, confocal line-scan is used to image the brain as 1-micrometer thin section cut by a diamond knife (image adapted from ref. 16). (**c**) In LSFM, the cleared brain is illuminated from the side with a light sheet (blue) through an illumination objective (or cylinder lens[19]) and imaged in a mosaic grid pattern from the top (image adapted from ref. 20). In all instruments, the brain is moved under the objective on a motorized *x-y-z* stage; PMT, photomultiplier tube.

combining anatomical and functional measurements are being applied to bridge the traditional structure-function divide in the study of the mammalian brain. In this Review, we aim to provide an overview of today's state of the art in LM instrumentation and to highlight the opportunities for progress as well as the challenges that need to be overcome to transform neuronal-tracing studies into a truly quantitative science that yields comprehensive descriptions of long-range and local projections and connectivity in whole mouse brains. We also discuss present strategies for the integration of anatomy and function in the study of mouse brain circuits.

Automated light microscopes for whole-brain imaging

The field of neuroanatomy has traditionally been associated with labor-intensive procedures that greatly limit the throughput of data collection. Recent efforts to automate LM instrumentation have standardized and dramatically increased the throughput of anatomical studies. The main challenge for these methods is to maintain the rigorous quality of traditional neuroanatomical studies, which results from detailed visual analysis, careful data collection and expert data interpretation.

There are currently two approaches to the automation of LM for imaging three-dimensional (3D) whole-brain data sets: one based on the integration of block-face microscopy and tissue sectioning and the other based on light-sheet fluorescence microscopy (LSFM) of chemically cleared tissue. The first approach has been developed for wide-field imaging, line-scan imaging, confocal microscopy and two-photon microscopy[8–16]. Common to all these instruments is the motorized movement of the sample under the microscope objective for top-view mosaic imaging, followed by mechanical removal of the imaged tissue before the next cycle of interleaved imaging and sectioning steps (**Fig. 1a**,**b**). As the objective is always near the tissue surface, it is possible to use high-numerical-aperture lenses to achieve submicrometer resolution close to the diffraction limits of LM.

Three instruments have been designed that combine two-photon microscopy[17] with subsequent tissue sectioning by ultrashort laser pulses in all-optical histology[10], by a milling machine in two-photon tissue cytometry[12] or by a vibrating blade microtome in serial two-photon (STP) tomography[15] (**Fig. 1a**). Whereas in both all-optical histology and two-photon tissue cytometry the sectioning obliterates the imaged tissue, the integration of vibratome-based sectioning in STP tomography allows the collection of the cut tissue for subsequent analysis by, for example, immunohistochemistry (see below). In addition, the tissue preparation by simple formaldehyde fixation and agar embedding in STP tomography has minimal detrimental effects on fluorescence and brain morphology. This makes STP tomography applicable to a broad range of neuroanatomical projects that use genetically encoded fluorescent protein–based tracers, which are sensitive to conditions used for fixation, dehydration and tissue clearing. This method is also versatile in terms of the mode and resolution of data collection. For example, imaging the mouse brain as a data set of 280 serial coronal sections, evenly spaced at 50 micrometers and at *x-y* resolution of 1 micrometer, takes about ~21 hours and generates a brain atlas–like data set of ~70 gigabytes. A complete visualization can be achieved by switching to 3D scanning of *z*-volume stacks between the mechanical sectioning steps, which allows the entire mouse brain to be imaged, for instance, at 1-micrometer *x-y* resolution and 2.5-micrometer *z* resolution in ~8 days, generating ~1.5 terabytes of data[15]. The instrument is commercially available from TissueVision Inc. The Allen Brain Institute is using this methodology for its Mouse Connectivity project (see below).

Two instruments have been designed to combine bright-field line-scan imaging and ultramicrotome sectioning of resin-embedded tissue in methods named knife-edge scanning microscopy (known as KESM)[13] and micro-optical sectioning tomography (MOST)[14] (**Fig. 1b**). The latter was used to image Golgi-stained mouse brain

at 0.33 × 0.33 × 1.0 micrometer *x-y-z* resolution, generating >8 terabytes of data in ~10 days[13,14]. The MOST instrument design was also recently built for fluorescence imaging (fMOST) by confocal laser scanning microscopy, with the throughput of one mouse brain at 1.0-micrometer voxel resolution in ~19 days[16]. Knife-edge scanning microscopy imaging is now also available as a commercial service from 3Scan.

The second approach for automated whole-brain imaging is based on LSFM (also known as selective-plane illumination microscopy[18] and ultramicroscopy[19]; **Fig. 1c**). This approach allows fast imaging of chemically cleared 'transparent' mouse brains without the need for mechanical sectioning[19,20] but, at least until now, with some trade-offs for anatomical tracing applications. The chemical clearing procedures reduced the signal of fluorescent proteins, but this problem appears to be solved by a new hydrogel-based tissue transformation and clearing method termed CLARITY[21] (see Perspective about this methodology in this Focus[22]). The spatial resolution of LSFM for the mouse brain also has been limited by the requirement for large field-of-view objectives with low power and low numerical aperture that were used to visualize the whole brain[19,23]. However, new objectives with long working distance and high numerical aperture, such as 8-millimeter working distance and 0.9 numerical aperture objective from Olympus, promise to enable LSFM of the whole mouse brain at submicrometer resolution. If necessary, LSFM can also be combined with one of several forms of structured illumination to reduce out-of-focus background fluorescence and improve contrast[24–26]. Taken together, these modifications are likely to enhance the applicability of LSFM to anterograde tracing of thin axons at high resolution in the whole mouse brain, as done by STP tomography in the AIBS Mouse Connectivity project (see below) and by fMOST in a recent report[16]. In addition, LSFM is well-suited for retrograde tracing in the mouse brain, which relies on detection of retrogradely fluorescence-labeled neuronal soma that are typically >10 micrometers in diameter. Such application was recently demonstrated for mapping retrograde connectivity of granule cells of the mouse olfactory bulb[20] using rabies viruses that achieve high levels of fluorescent protein labeling[27,28].

Mesoscopic connectivity-mapping projects

The labeling of neurons and subsequent neuroanatomical tract tracing by LM methods has been used for over a century to interrogate the anatomical substrate of the transmission of information in the brain. Throughout those years, the credo of neuroanatomy, 'the gain in brain is mainly in the stain', signified that progress was made mainly through the development of new anatomical tracers. Yet despite the decades of neuroanatomical research, the laborious nature of tissue-processing and data-visualization has kept the progress in our knowledge of brain circuitry at a disappointingly slow pace[7]. Today, neuroanatomy stands to greatly benefit from the application of high-throughput automated LM instruments and powerful informatics tools for the analysis of mouse brain data[29,30]. The high-resolution capacity LM methods afford, and the fact that an entire brain data set can be captured, makes these systems well-suited for the systematic charting of the spatial profile and the connectivity of populations of neurons and even individual cells projecting over long distances.

The pioneering effort in the field of anatomical projects applied at the scale of whole animal brains was the Allen Mouse Brain Atlas of Gene Expression, which cataloged *in situ* hybridization maps for more than 20,000 genes in an online 3D digital mouse brain atlas[29,31,32]. The proposal by a consortium of scientists led by Partha Mitra to generate similar LM-based atlases of 'brain-wide neuroanatomical connectivity' in several animal models[7] has in short time spurred three independent projects, each promising to trace all efferent and afferent anatomical pathways in the mouse brain. The aim of the Mouse Brain Architecture Project (http://brainarchitecture.org/) from the Mitra team at CSHL is to image >1,000 brains; the Allen Mouse Brain Connectivity Atlas project (http://connectivity.brain-map.org/) led by Hongkui Zeng at AIBS has a goal of imaging >2,000 brains; and the Mouse Connectome Project (http://www.mouseconnectome.org/) led by Hong-Wei Dong at UCLA has a goal of imaging 500 brains, with each brain injected with four tracers. Whereas the CSHL and UCLA projects rely on automated wide-field fluorescence microscopy (Hamamatsu Nanozoomer 2.0 and Olympus VS110, respectively) to image manually sectioned brains, the Mouse Connectivity project at the Allen Institute is being done entirely by STP tomography[15]. The main strength of these efforts is in the broad range of tracers used. Given that each tracer has its own advantages and problems[33], the information derived from all three projects will ensure generalizable interpretation of the projection results throughout the brain. The CSHL group uses a combination of traditional anterograde and retrograde tracers, fluorophore-conjugated dextran amine[34] and cholera toxin B (CTB) subunit[35], respectively, which are complemented by a combination of viral vector–based tracers, GFP-expressing adeno-associated virus (AAV)[36] for anterograde tracing (**Fig. 2a**) and modified rabies virus[27] for retrograde tracing. Although the virus-based methods are less well tested, they offer advantages in terms of the brightness of labeling and the possibility of cell type–specific targeting using Cre recombinase–dependent viral vectors[37] and transgenic lines expressing Cre recombinase from cell type–specific promoters[38–40]. The AIBS team uses solely anterograde tracing by AAV-GFP viruses that label axonal arborizations with GFP[41] (**Fig. 2b**), in many cases taking advantage of transgenic 'driver' mouse lines expressing Cre recombinase from cell type–specific promoters to achieve anterograde tracing of specific neuronal cell types. Finally, the team at UCLA is using a strategy of two injections per brain, each with a mix of anterograde and retrograde tracers[42]: CTB together with *Phaseolus vulgaris* leucoagglutinin[43] and FluoroGold[44] together with biotinylated dextran amine[42,45]. This approach has an added advantage of enabling direct visualization of the convergence of inputs and outputs from across different areas in one brain[42,46,47].

The unprecedented amounts of data being collected in these projects means that the considerable person-hours historically spent performing microscopy have largely shifted toward data analysis. The first step of such data analysis comprises the compilation of the serial section images for viewing as whole-brain data sets at resolutions beyond the minimum geometric volume of the neuronal structures of interest: soma for retrograde tracing and axons for anterograde tracing. All three projects offer a convenient way to browse the data sets online, including high-resolution magnified views that in most cases are sufficient to visually determine labeled soma and axons. All three projects use the Allen

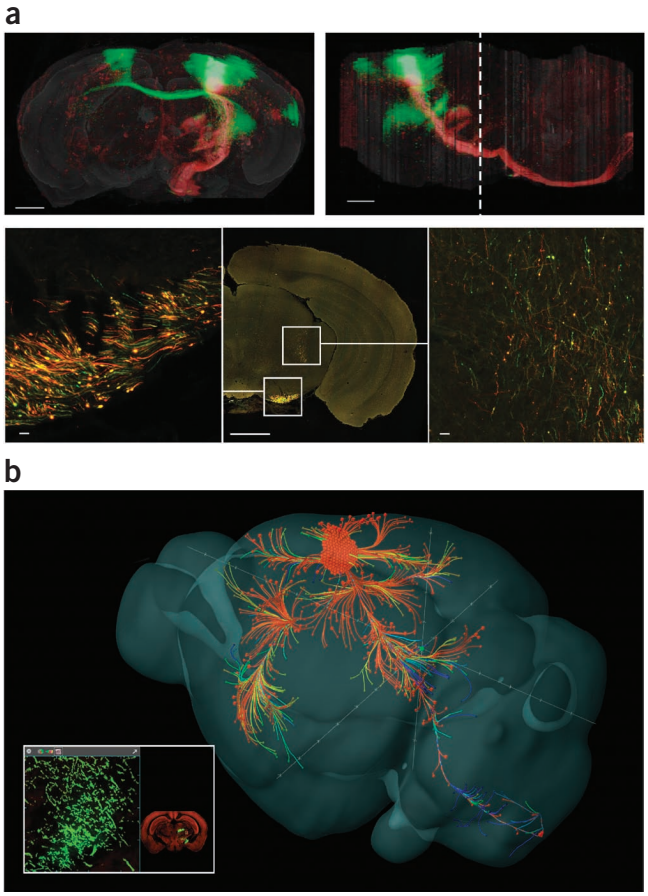

Figure 2 | Primary motor cortex projection maps. (**a**) Mouse Brain Architecture data of AAV-GFP injected into the supragranular layers and AAV–red fluorescent protein injected in the infragranular layers (F. Mechler and P. Mitra; unpublished data). Front (left) and lateral (right) views of the volume-rendered brain (top); and coronal section image from the area marked by the dashed line (center) with magnification of the lower boxed region showing axonal fibers in the cerebral peduncle (left) and magnification of the upper boxed region showing projections to the midbrain reticular nucleus (right). Scale bars, 1,000 µm (top) and 20 µm (bottom). (**b**) Mouse Connectivity data of a similar AAV-GFP injection show the primary motor cortex projectome reconstructed in the Allen Brain Explorer[48] (H. Zeng; unpublished data). Inset, magnified view and coronal section overview of projections in the ventral posteromedial (VPM) nucleus of the thalamus.

Mouse Brain Atlas for the registration of the coronal sections, which will help in the cross-validation of results obtained from the different tracers. The Allen Mouse Brain Connectivity Atlas website also offers the option to view the data after projection segmentation, which selectively highlights labeled axons, as well as in 3D in the Brain Explorer registered to the Allen Mouse Brain Atlas[48] (**Fig. 2b**).

The second step of data analysis requires the development of informatics methods for quantitation of the data sets, which will facilitate the interpretation of the data available online. The Allen Mouse Brain Connectivity Atlas online tools allow the user to search the projections between injected regions and display the labeled pathways as tracks in three dimensions in the Brain Explorer. The CSHL and UCLA connectomes can currently be viewed online as serial section data sets. The data from the Cre recombinase driver mouse lines in the AIBS project provide a unique feature of cell-type specificity for the interpretation of the anterograde projections. The main strength of the CSHL and UCLA efforts lies in the multiplicity of the anatomical tracers used. The use of multiple retrograde tracers in particular will yield useful information, as retrogradely labeled soma (>10 micrometers in diameter) are easier to quantify than thin (<1 micrometer) axon fibers. These experiments will also provide an important comparison between the traditional CTB and FluoroGold tracers and the rabies virus tracer that is also being used in trans-synaptic labeling (see below) but is less well studied and may show some variation in transport affinity at different types of synapses. In summary, the LM-based mesoscopic mapping projects are set to transform the study of the circuit wiring of the mouse brain by providing online access to whole-brain data sets from several thousand injections of anterograde and retrograde tracers. The informatics tools being developed to search the databases will greatly aid in parsing the large amounts of data and in accessing specific brain samples for detailed scholarly analyses by the neuroscience community.

Mapping connectivity using trans-synaptic tracers

In contrast to electron microscopy methods, which provide a readout of neuronal connectivity with synapse resolution over small volumes of tissue, the whole-brain LM methods permit the assessment of projection-based connectivity between brain regions and in some cases between specific cell types in those regions but without the option of visualizing the underlying synaptic contacts. Trans-synaptic viruses that cross either multiple or single synapses can help to circumvent the requirement to confirm connectivity at resolution achieved by electron microscopy because such connectivity may be inferred from the known direction and mechanism of spread of the trans-synaptic tracer. Trans-synaptic tracers based on rabies virus, pseudorabies virus and herpes simplex virus, which repeatedly cross synaptic connections in a retrograde or anterograde direction, are powerful tools for studying multistep pathways upstream and downstream from the starter cell population[49–51]. Furthermore, modified trans-synaptic rabies viruses have been developed that are restricted in their spread to a single synaptic jump and thus can be used to identify monosynaptic connections onto and downstream of specific neuronal populations and even individual cells[27,52–58] (**Fig. 3**).

Rabies virus spreads from the initially infected cells in a trans-synaptic retrograde manner[49,59]. Rabies virus infection does not occur via spurious spread or uptake by fibers of passage and, because it cannot cross via electrical synapses, it is an effective tool for unidirectional anatomical tracing[60]. In a modified rabies virus system, the infection can also be cell type–targeted by encapsulating glycoprotein-deficient rabies virus with an avian virus envelope protein (referred to as 'SAD-ΔG-EnvA'). This restricts infection to only those cells that express an avian receptor protein TVA that is natively found in birds but not in mammals[61,62]. Thus, the delivery of vectors driving the expression of both TVA and rabies virus glycoprotein (RV-G) into a single cell[28,54,56] (see below) or a specific population of cells[55,63], ensures that only the targeted cell or cells will (i) be susceptible to initial infection and (ii) provide the replication-incompetent virus with RV-G required for trans-synaptic infection[64]. In this system, the virus can spread from the primarily infected cell or cells to the presynaptic

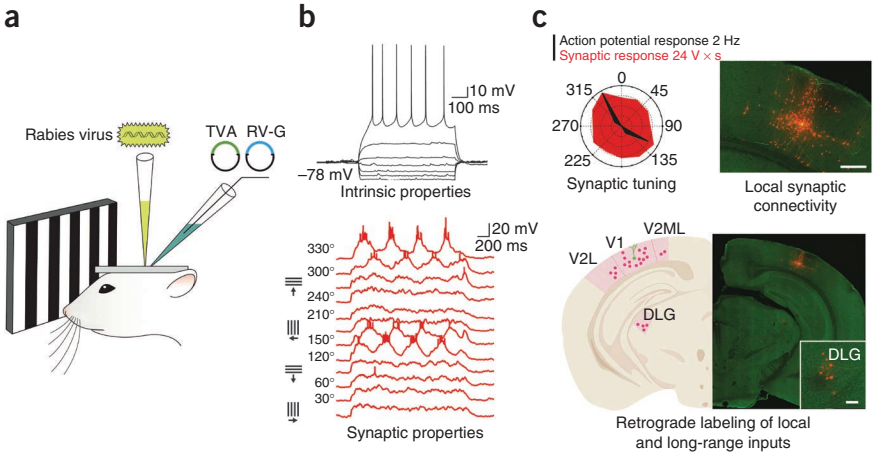

Figure 3 | Mapping the function and connectivity of single cells in the mouse brain *in vivo*. (**a**) Experimental setup for combined single-cell physiology and trans-synaptic connectivity mapping. Patch pipettes have solutions containing DNA vectors used to drive the expression of the TVA and RV-G proteins. (**b**) Patch pipettes are used to perform a whole-cell recording of the intrinsic and sensory-evoked synaptic properties of a single layer-5 neuron in primary visual cortex. Synaptic responses are averages of five traces. (**c**) Then the encapsulated modified rabies virus is injected into the brain in close proximity to the recorded neuron. After a period of up to 12 days to ensure retrograde spread of the modified rabies from the recorded neuron, the brain is removed and imaged for identification of the local and long-range presynaptic inputs underlying the tuning of the recorded neuron to the direction of visual motion (polar plot). Fluorescence image on the right shows injection site with the starter cell (yellow) in the middle. Scheme (bottom left) and imaged data (bottom right) of long-range retrograde tracing. V1, primary visual cortex; V2L, secondary visual cortex (lateral); V2ML secondary visual cortex (medio-lateral). Inset shows long-range inputs from the dorsal lateral geniculate nucleus (DLG). Scale bars, 300 μm (top) and 50 μm (bottom), respectively. Images modified from ref. 54.

input cells, which become labeled by expression of a fluorescent protein. However, as the presynaptic cells do not express RV-G[28], the virus cannot spread further. This approach thus allows the discovery of the identity and location of the upstream input network relative to a defined population of neurons[57,58].

Brain-region specificity and cell-type specificity for mapping connectivity by the modified rabies virus system can be achieved by using a Cre recombinase–dependent helper virus driving expression of TVA and RV-G and transgenic driver mouse lines that express Cre recombinase in specific cell types or cortical layers[38,39,63]. This strategy is particularly useful for brain regions comprising many different cell types that could not be otherwise selectively targeted. Moreover, the engineering of other neurotropic trans-synaptic viruses is adding new tools for anatomical tracing, including Cre recombinase–dependent anterograde tracers based on a modified H129 strain of herpes simplex virus[65] and vesicular stomatitis virus[66], and retrograde tracers based on a modified pseudorabies virus (H. Oyibo and A. Zador, personal communication). The use of retrograde and anterograde trans-synaptic viruses, in combination with whole-brain LM methods, thus promises to afford unprecedented access to the upstream and downstream connectivity of specific cell types in the mouse brain.

Present challenges and opportunities for whole-brain LM

As highlighted above, LM instruments for whole-brain imaging are expected to make a substantial contribution in large-scale projects that focus on anatomical connectivity at the level of the whole mouse brain. It has also become clear that the use of these instruments will have an impact in many experimental applications in different neuroscience laboratories. It is therefore imperative that there exist broadly applicable image-processing, warping and analytical tools that will facilitate data sharing and across-laboratory collaboration and validation in future neuroscience studies focusing on, for example, mapping whole-brain anatomical changes during development and in response to experience.

One practical problem arising from the choice to scan entire mouse brains at high resolution relates to the handling of large data sets (up to several terabytes per brain), which necessitates automated analytical pipelining. STP tomography is currently the most broadly used method among the whole-brain LM approaches, and there are freely available informatics tools for compiling STP tomography image stacks and viewing them as three-dimensional data, including algorithms that automate seamless stitching[15]. Another key challenge for charting the distribution of the labeled elements in the whole mouse brain is the process of accurate registration of the individual brain data sets onto an anatomical reference atlas. To this end, scientists at AIBS have generated the open-source segmented Allen Mouse Brain Atlas for the adult C57BL/6 mouse[29,31,32,48], which is also available for registration of data sets generated by STP tomography (**Figs. 2b** and **4b**). In addition, the so-called Waxholm space for standardized digital atlasing[67] allows comparisons of registered mouse brain data using multiple brain atlases, including the Allen Mouse Brain Atlas, the digital Paxinos and Franklin Mouse Brain Atlas[68], and several magnetic resonance imaging reference mouse brains. The continuing development of the Waxholm space and other online data-analysis platforms[30,69,70] will be essential for standardized comparisons of mouse brain data collected in different laboratories using different instruments.

The completion of the three mesoscopic connectome projects in the next several years will yield a comprehensive map of point-to-point connectivity between anatomical regions in the mouse brain[7]. Determining the cell-type identity of the neurons sending and receiving the connections in the brain regions will be essential for interpreting the function of the brain-wide neural circuits. Immunohistochemical analyses of labeled circuits have proven invaluable for ascertaining the identity of specific classes of neurons[71–73] and synaptic connections[52,74]. The combination of immunohistochemical analysis by array tomography[75,76] and anatomical tracing by the whole-brain LM instruments promises to be particularly powerful, as it will bring together two largely automated methodologies with complementary focus on synaptic and mesoscopic connectivity, respectively. STP tomography outputs sectioned tissue (typically 50-micrometer-thick sections[15]), which can be further resectioned, processed and reimaged by array

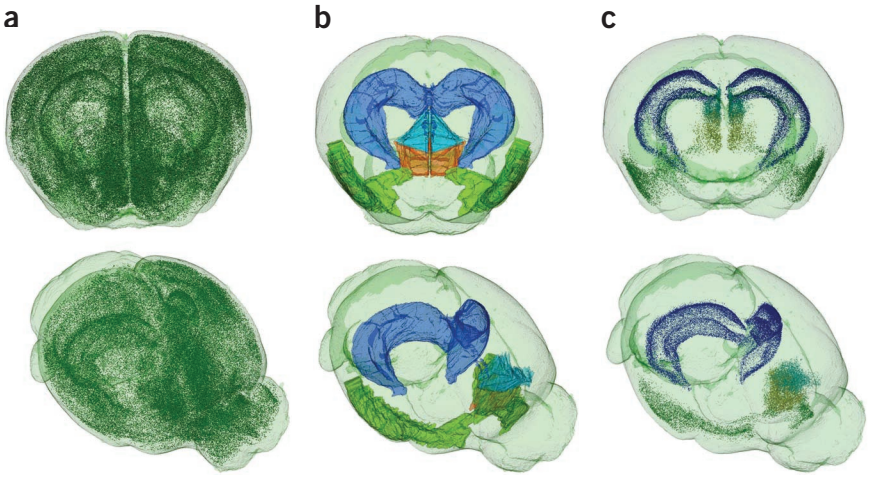

Figure 4 | Imaging induction of c-fos as a means to map whole-brain activation. (**a**) A 3D visualization of 367,378 c-fos–GFP cells detected in 280 coronal sections of an STP tomography data set of a mouse brain after the mouse was allowed to explore a novel object for 90 seconds. (**b**) Examples of anatomical segmentation of the brain volume with the Allen Mouse Brain Reference Atlas labels[48] modified for the 280-section STP tomography data sets: hippocampus (blue), prelimbic cortex (aqua), infralimbic cortex (orange) and piriform cortex (green). (**c**) Visualization of c-fos–GFP cells in the hippocampus (38,170 cells), prelimbic cortex (3,305 cells), infralimbic cortex (3,827 cells) and piriform cortex (10,910 cells) (P.O., Y. Kim and K. Umadevi Venkataraju; unpublished data).

tomography for integrating cell type–specific information into the whole-brain data sets. Industrial-level automation of slice capture and immunostaining can be developed to minimize manual handling and enhance the integration of immunohistochemistry and STP tomography. In addition, sectioning and immunostaining can also be applied to LSFM-imaged mouse brains[20].

A related, cell type–focused application of whole-brain LM imaging will be to quantitatively map the distribution (the cell counts) of different neuronal cell types in all anatomical regions in the mouse brain. Several such cell count–based anatomical studies have been done previously at smaller scales, revealing, for example, cell densities with respect to cortical vasculature[77] or the density of neuronal cell types per layer in a single cortical column[78–80]. Using the whole-brain LM methods, a comprehensive anatomical atlas of different GABAergic inhibitory interneurons[81] can now be generated by imaging cell type–specific Cre recombinase–mediated knock-in mouse lines[38,39] crossed with Cre recombinase–dependent reporter mice expressing nuclear GFP. These and similar data sets for other neuronal cell types will complement the mesoscopic brain region connectivity data and help the interpretation of the immunohistochemistry data by providing a reference for total numbers of specific cell types per anatomical brain region.

Integrating brain anatomy and function

The anterograde, retrograde and trans-synaptic tracing approaches described above will yield the structural scaffold of anatomical projections and connections throughout the mouse brain. However, such data will not be sufficient to identify how specific brain regions connect to form functional circuits driving different behaviors. Bridging whole-brain structure and function is the next frontier in systems neuroscience, and the development of new technologies and methods will be crucial in achieving progress.

The structure-function relationship of single neurons can be examined by *in vivo* intracellular delivery of the DNA vectors required for targeting and driving trans-synaptic virus expression via patch pipettes in loose cell-attached mode for electroporation[56] or via whole-cell recording[54] (**Fig. 3**). Used in combination with two-photon microscopy, this single-cell delivery technique may also be targeted at fluorescently labeled neurons of specific cell types[56,82,83]. The whole-cell method is particularly informative, as its intracellular nature permits recording the intrinsic biophysical profile of the target cell, which, in turn, may reflect its functional connectivity status in the local network[84]. In addition, by recording sensory-evoked inputs, it is possible to compare single-cell synaptic receptive fields and anatomical local and long-range connectivity traced by LM methods[54]. This combinatorial approach, involving single-cell electrophysiology and genetic manipulation designed for connection mapping, makes it possible to test long-standing theories regarding the extent to which emergent features of sensory cortical function manifest via specific wiring motifs[85].

As has recently been achieved for serial electron microscopy–based reconstruction[86,87], it will also be valuable to functionally characterize larger local neuronal populations for registration against LM-based connectivity data. In this sense, genetically encoded calcium indicators, which permit physiological characterization of neuronal activity in specific cell types[88–90], along with viral vectors for trans-synaptic labeling and LM-based tracing, will have critical complementary roles. Large-volume *in vivo* two-photon imaging of neuronal activity before *ex vivo* whole-brain imaging will establish the extent to which connectivity patterns relate to function[91] at the level of single cells, and local and long-range circuits. Interpolation of such experiments will rely on the ability to cross-register *in vivo* functional imaging with complete *ex vivo* LM connectivity data. Preliminary experiments, which already hint at the spatial spread of monosynaptic connectivity of individual principal cortical cells, suggest that combination of functional imaging and traditional anatomical-circuit reconstruction may only be feasible at the local network level where connection probability is the highest[92–94]. Given the broad, sparse expanse of connectivity in most brain regions and especially in cortical areas, high-throughput whole-brain LM methods will be imperative for complete anatomical-circuit reconstruction of functionally characterized local networks.

The amalgamation of whole-brain LM and physiological methods for single neurons and small networks offers a powerful means to study the mouse brain. An exciting application of this approach will be to trace the synaptic circuits of neurons functionally characterized in head-fixed behaving animals engaged in tasks related to spatial navigation, sensorimotor integration and other complex brain functions[95–97]. This research will lead to the generation of whole-brain structure-function hypotheses for specific

behaviors, which can then be tested for causality by optogenetic methods targeted to the identified cell types and brain regions[98]. Furthermore, LM, physiological and optogenetic methods can be applied to interrogate entire brain systems in large-scale projects, as is currently being done for the mouse visual cortex in an effort led by C. Koch and R.C. Reid at AIBS[99].

Finally, a discussion in the neuroscience community has been initiated regarding the feasibility of mapping activity at cellular resolution in whole brains and linking the identified activity patterns to brain anatomy[100]. Today, such experiments are possible in small, transparent organisms, as was demonstrated by two-photon microscopy and LSFM-based imaging of brain activity in larval zebrafish expressing the calcium indicator GCaMP[89,101,102]. Understandably, LM-based approaches will not be useful for *in vivo* whole-brain imaging in larger, nontransparent animals, and the invention of new disruptive technologies will likely be needed to achieve the goal of mapping real-time brain activity at cellular resolution in, for example, the mouse. In contrast, LM methods can be used to map patterns of whole-brain activation indirectly, by post-*hoc* visualization of activity-induced expression of immediate early genes, such as mouse *Fos* (*c-fos*), *Arc* or *Homer1a* (ref. 103). Transgenic fluorescent immediate early gene reporter mice, such as c-fos–GFP or Arc-GFP mice[104–106], can be trained in a specific behavior, their brains subsequently can be imaged *ex vivo*, and the exact distribution of GFP-positive neurons can be mapped and analyzed by computational methods (**Fig. 4**). In this approach, a statistical analysis of the counts of GFP-labeled neurons can be used to identify brain regions and cell types activated during behaviors but without providing information on the temporal sequence of brain region activation or the firing patterns of the activated cells. However, the development of more sensitive, for instance, fluorescent RNA–based methods, may allow calibration of the cellular signal with respect to the temporal window and the pattern of activity related to the induction of immediate early genes. Such calibration would considerably enhance the power of LM-based whole-brain mapping of the induction of immediate early genes, which, in combination with the connectomics data, could then be used to begin to build cellular-resolution models of function-based whole-brain circuits.

Conclusions

The advances in automated LM methods, anatomical tracers, physiological methods and informatics tools have begun to transform our understanding of the circuit wiring in the mouse brain. The focus on the mouse as an animal model is, of course, not accidental. In addition to the generation of cell type–specific driver mouse lines[38–40] that allow the study of specific neuronal populations in the normal brain, mouse genetics are used in hundreds of laboratories to model gene mutations linked to heritable human disorders, including complex cognitive disorders such as autism and schizophrenia. Without a doubt, understanding the relationships between brain structure and function in the genetic mouse models will be crucial to understanding the underlying brain circuit mechanisms of these disorders. The toolbox of LM methods described here, and the continuing development of new methods, promise to transform the study of brain circuits in animal models and to decipher the structure-function relationships essential to the understanding of complex brain functions and their deficits in human brain disorders.

ACKNOWLEDGMENTS

We thank P. Mitra, H. Zeng and Christian Niedworok for comments on the manuscript and J. Kuhl for the graphics. P.O. is supported by the US National Institute of Mental Health grant 1R01MH096946-01, McKnight Foundation, Technological Innovations in Neuroscience Award and Simons Foundation for Autism Research grants 204719 and 253447. T.W.M. is supported as a Wellcome Trust Investigator and by the Medical Research Council MC U1175975156.

COMPETING FINANCIAL INTERESTS

The authors declare competing financial interests: details are available in the online version of the paper.

1. Golgi, C. *Sulla Struttura Della Sostanza Grigia del Cervello*. *Gazz. Med. Ital. (Lombardia)* **33**, 244–246 (1873).
2. Ramón y Cajal, S. *Textura del Sistema Nervioso del Hombre y de los Vertebrados*. Vol. 2 (Moya, 1904).
3. Felleman, D.J. & Van Essen, D.C. Distributed hierarchical processing in the primate cerebral cortex. *Cereb. Cortex* **1**, 1–47 (1991).
4. Rockland, K.S. & Pandya, D.N. Laminar origins and terminations of cortical connections of the occipital lobe in the rhesus monkey. *Brain Res.* **179**, 3–20 (1979).
5. Craddock, R.C. *et al.* Imaging human connectomes at the macroscale. *Nat. Methods* **10**, 524–539 (2013).
6. Helmstaedter, M. Cellular-resolution connectomics: challenges of dense neural circuit reconstruction. *Nat. Methods* **10**, 501–507 (2013).
7. Bohland, J.W. *et al.* A proposal for a coordinated effort for the determination of brainwide neuroanatomical connectivity in model organisms at a mesoscopic scale. *PLoS Comput. Biol.* **5**, e1000334 (2009).
This paper describes the rationale for mapping connectivity in the whole mouse brain at the mesoscale level by LM.
8. Odgaard, A., Andersen, K., Melsen, F. & Gundersen, H.J. A direct method for fast three-dimensional serial reconstruction. *J. Microsc.* **159**, 335–342 (1990).
9. Ewald, A.J., McBride, H., Reddington, M., Fraser, S.E. & Kerschmann, R. Surface imaging microscopy, an automated method for visualizing whole embryo samples in three dimensions at high resolution. *Dev. Dyn.* **225**, 369–375 (2002).
10. Tsai, P.S. *et al.* All-optical histology using ultrashort laser pulses. *Neuron* **39**, 27–41 (2003).
This study pioneered the approach of serial imaging by two-photon microscopy and tissue sectioning for *ex vivo* collection of neuroanatomical data.
11. Sands, G.B. *et al.* Automated imaging of extended tissue volumes using confocal microscopy. *Microsc. Res. Tech.* **67**, 227–239 (2005).
12. Ragan, T. *et al.* High-resolution whole organ imaging using two-photon tissue cytometry. *J. Biomed. Opt.* **12**, 014015 (2007).
13. Mayerich, D., Abbott, L. & McCormick, B. Knife-edge scanning microscopy for imaging and reconstruction of three-dimensional anatomical structures of the mouse brain. *J. Microsc.* **231**, 134–143 (2008).
14. Li, A. *et al.* Micro-optical sectioning tomography to obtain a high-resolution atlas of the mouse brain. *Science* **330**, 1404–1408 (2010).
15. Ragan, T. *et al.* Serial two-photon tomography for automated *ex vivo* mouse brain imaging. *Nat. Methods* **9**, 255–258 (2012).
This study introduces the method of STP tomography and demonstrates its use for anterograde and retrograde tracing in the mouse brain.
16. Gong, H. *et al.* Continuously tracing brain-wide long-distance axonal projections in mice at a one-micron voxel resolution. *Neuroimage* **74**, 87–98, (2013).
This study demonstrates the first long-range tracing of individual axons in the mouse brain by fMOST.
17. Denk, W., Strickler, J.H. & Webb, W.W. Two-photon laser scanning fluorescence microscopy. *Science* **248**, 73–76 (1990).
18. Huisken, J., Swoger, J., Del Bene, F., Wittbrodt, J. & Stelzer, E.H. Optical sectioning deep inside live embryos by selective plane illumination microscopy. *Science* **305**, 1007–1009 (2004).
19. Dodt, H.U. *et al.* Ultramicroscopy: three-dimensional visualization of neuronal networks in the whole mouse brain. *Nat. Methods* **4**, 331–336 (2007).
This study is the first to use LSFM for imaging the entire mouse brain.

20. Niedworok, C.J. *et al.* Charting monosynaptic connectivity maps by two-color light-sheet fluorescence microscopy. *Cell Rep.* **2**, 1375–1386 (2012).
21. Chung, K. *et al.* Structural and molecular interrogation of intact biological systems. *Nature* doi:10.1038/nature12107 (2013).
22. Chung, K. & Deisseroth, K. CLARITY for mapping the nervous system. *Nat. Methods* **10**, 508–513 (2013).
23. Leischner, U., Zieglgansberger, W. & Dodt, H.U. Resolution of ultramicroscopy and field of view analysis. *PLoS ONE* **4**, e5785 (2009).
24. Mertz, J. & Kim, J. Scanning light-sheet microscopy in the whole mouse brain with HiLo background rejection. *J. Biomed. Opt.* **15**, 016027 (2010).
25. Kalchmair, S., Jahrling, N., Becker, K. & Dodt, H.U. Image contrast enhancement in confocal ultramicroscopy. *Opt. Lett.* **35**, 79–81 (2010).
26. Keller, P.J. *et al.* Fast, high-contrast imaging of animal development with scanned light sheet-based structured-illumination microscopy. *Nat. Methods* **7**, 637–642 (2010).
27. Wickersham, I.R., Finke, S., Conzelmann, K.K. & Callaway, E.M. Retrograde neuronal tracing with a deletion-mutant rabies virus. *Nat. Methods* **4**, 47–49 (2007).
28. Wickersham, I.R. *et al.* Monosynaptic restriction of transsynaptic tracing from single, genetically targeted neurons. *Neuron* **53**, 639–647 (2007).
This study describes a genetically modified rabies virus designed to specifically label direct presynaptic input onto a given cell population.
29. Ng, L. *et al.* An anatomic gene expression atlas of the adult mouse brain. *Nat. Neurosci.* **12**, 356–362 (2009).
30. Jones, E.G., Stone, J.M. & Karten, H.J. High-resolution digital brain atlases: a Hubble telescope for the brain. *Ann. NY Acad. Sci.* **1225** (suppl. 1), E147–E159 (2011).
31. Lein, E.S. *et al.* Genome-wide atlas of gene expression in the adult mouse brain. *Nature* **445**, 168–176 (2007).
This study pioneered large-scale LM-based mouse brain anatomy and introduced the Allen Mouse Brain Atlas and online data portal.
32. Dong, H.W. *The Allen Reference Atlas: A Digital Color Brain Atlas of the C57Bl/6J Male Mouse* (John Wiley & Sons Inc., 2008).
33. Lanciego, J.L. & Wouterlood, F.G. A half century of experimental neuroanatomical tracing. *J. Chem. Neuroanat.* **42**, 157–183 (2011).
34. Glover, J.C., Petursdottir, G. & Jansen, J.K. Fluorescent dextran-amines used as axonal tracers in the nervous system of the chicken embryo. *J. Neurosci. Methods* **18**, 243–254 (1986).
35. Llewellyn-Smith, I.J., Martin, C.L., Arnolda, L.F. & Minson, J.B. Tracer-toxins: cholera toxin B-saporin as a model. *J. Neurosci. Methods* **103**, 83–90 (2000).
36. Grinevich, V., Brecht, M. & Osten, P. Monosynaptic pathway from rat vibrissa motor cortex to facial motor neurons revealed by lentivirus-based axonal tracing. *J. Neurosci.* **25**, 8250–8258 (2005).
37. Atasoy, D., Aponte, Y., Su, H.H. & Sternson, S.M. A FLEX switch targets Channelrhodopsin-2 to multiple cell types for imaging and long-range circuit mapping. *J. Neurosci.* **28**, 7025–7030 (2008).
38. Taniguchi, H. *et al.* A resource of Cre driver lines for genetic targeting of GABAergic neurons in cerebral cortex. *Neuron* **71**, 995–1013 (2011).
39. Madisen, L. *et al.* A robust and high-throughput Cre reporting and characterization system for the whole mouse brain. *Nat. Neurosci.* **13**, 133–140 (2010).
40. Madisen, L. *et al.* A toolbox of Cre-dependent optogenetic transgenic mice for light-induced activation and silencing. *Nat. Neurosci.* **15**, 793–802 (2012).
41. Harris, J.A., Wook Oh, S. & Zeng, H. Adeno-associated viral vectors for anterograde axonal tracing with fluorescent proteins in nontransgenic and cre driver mice. *Curr. Protoc. Neurosci.* **1.20**, 21–18 (2012).
42. Thompson, R.H. & Swanson, L.W. Hypothesis-driven structural connectivity analysis supports network over hierarchical model of brain architecture. *Proc. Natl. Acad. Sci. USA* **107**, 15235–15239 (2010).
43. Gerfen, C.R. & Sawchenko, P.E. An anterograde neuroanatomical tracing method that shows the detailed morphology of neurons, their axons and terminals: immunohistochemical localization of an axonally transported plant lectin, *Phaseolus vulgaris* leucoagglutinin (PHA-L). *Brain Res.* **290**, 219–238 (1984).
44. Naumann, T., Hartig, W. & Frotscher, M. Retrograde tracing with Fluoro-Gold: different methods of tracer detection at the ultrastructural level and neurodegenerative changes of back-filled neurons in long-term studies. *J. Neurosci. Methods* **103**, 11–21 (2000).
45. Reiner, A. *et al.* Pathway tracing using biotinylated dextran amines. *J. Neurosci. Methods* **103**, 23–37 (2000).
46. Hintiryan, H. *et al.* Comprehensive connectivity of the mouse main olfactory bulb: analysis and online digital atlas. *Front. Neuroanat.* **6**, 30 (2012).
47. Conte, W.L., Kamishina, H. & Reep, R.L. Multiple neuroanatomical tract-tracing using fluorescent Alexa Fluor conjugates of cholera toxin subunit B in rats. *Nat. Protoc.* **4**, 1157–1166 (2009).
48. Sunkin, S.M. *et al.* Allen Brain Atlas: an integrated spatio-temporal portal for exploring the central nervous system. *Nucleic Acids Res.* **41**, D996–D1008 (2013).
49. Ugolini, G. Advances in viral transneuronal tracing. *J. Neurosci. Methods* **194**, 2–20 (2010).
50. Ekstrand, M.I., Enquist, L.W. & Pomeranz, L.E. The alpha-herpesviruses: molecular pathfinders in nervous system circuits. *Trends Mol. Med.* **14**, 134–140 (2008).
51. Song, C.K., Enquist, L.W. & Bartness, T.J. New developments in tracing neural circuits with herpesviruses. *Virus Res.* **111**, 235–249 (2005).
52. Callaway, E.M. Transneuronal circuit tracing with neurotropic viruses. *Curr. Opin. Neurobiol.* **18**, 617–623 (2008).
53. Wickersham, I.R. & Feinberg, E.H. New technologies for imaging synaptic partners. *Curr. Opin. Neurobiol.* **22**, 121–127 (2012).
54. Rancz, E.A. *et al.* Transfection via whole-cell recording *in vivo*: bridging single-cell physiology, genetics and connectomics. *Nat. Neurosci.* **14**, 527–532 (2011).
This study was the first to combine intracellular neuronal recording with DNA delivery. The authors use this method to map the synaptic function of a single cell *in vivo* and then target rabies-based retrograde labeling of the cells' synaptic input.
55. Miyamichi, K. *et al.* Cortical representations of olfactory input by trans-synaptic tracing. *Nature* **472**, 191–196 (2011).
56. Marshel, J.H., Mori, T., Nielsen, K.J. & Callaway, E.M. Targeting single neuronal networks for gene expression and cell labeling *in vivo*. *Neuron* **67**, 562–574 (2010).
This paper describes an electroporation method for single-cell delivery of DNA for targeted infection of modified rabies virus.
57. Takatoh, J. *et al.* New modules are added to vibrissal premotor circuitry with the emergence of exploratory whisking. *Neuron* **77**, 346–360 (2013).
58. Arenkiel, B.R. *et al.* Activity-induced remodeling of olfactory bulb microcircuits revealed by monosynaptic tracing. *PLoS ONE* **6**, e29423 (2011).
59. Finke, S. & Conzelmann, K.K. Replication strategies of rabies virus. *Virus Res.* **111**, 120–131 (2005).
60. Ugolini, G. Specificity of rabies virus as a transneuronal tracer of motor networks: transfer from hypoglossal motoneurons to connected second-order and higher order central nervous system cell groups. *J. Comp. Neurol.* **356**, 457–480 (1995).
61. Federspiel, M.J., Bates, P., Young, J.A., Varmus, H.E. & Hughes, S.H. A system for tissue-specific gene targeting: transgenic mice susceptible to subgroup A avian leukosis virus-based retroviral vectors. *Proc. Natl. Acad. Sci. USA* **91**, 11241–11245 (1994).
62. Young, J.A., Bates, P. & Varmus, H.E. Isolation of a chicken gene that confers susceptibility to infection by subgroup A avian leukosis and sarcoma viruses. *J. Virol.* **67**, 1811–1816 (1993).
63. Wall, N.R., Wickersham, I.R., Cetin, A., De La Parra, M. & Callaway, E.M. Monosynaptic circuit tracing *in vivo* through Cre-dependent targeting and complementation of modified rabies virus. *Proc. Natl. Acad. Sci. USA* **107**, 21848–21853 (2010).
64. Etessami, R. *et al.* Spread and pathogenic characteristics of a G-deficient rabies virus recombinant: an *in vitro* and *in vivo* study. *J. Gen. Virol.* **81**, 2147–2153 (2000).
65. Lo, L. & Anderson, D.J.A. Cre-dependent, anterograde transsynaptic viral tracer for mapping output pathways of genetically marked neurons. *Neuron* **72**, 938–950 (2011).
66. Beier, K.T. *et al.* Anterograde or retrograde transsynaptic labeling of CNS neurons with vesicular stomatitis virus vectors. *Proc. Natl. Acad. Sci. USA* **108**, 15414–15419 (2011).
67. Hawrylycz, M. *et al.* Digital atlasing and standardization in the mouse brain. *PLoS Comput. Biol.* **7**, e1001065 (2011).
68. Paxinos, G. & Franklin, K.B. *The Mouse Brain in Stereotaxic Coordinates* (Gulf Professional Publishing, 2004).
69. Swanson, L.W. & Bota, M. Foundational model of structural connectivity in the nervous system with a schema for wiring diagrams, connectome, and basic plan architecture. *Proc. Natl. Acad. Sci. USA* **107**, 20610–20617 (2010).

70. Moene, I.A., Subramaniam, S., Darin, D., Leergaard, T.B. & Bjaalie, J.G. Toward a workbench for rodent brain image data: systems architecture and design. *Neuroinformatics* **5**, 35–58 (2007).
71. Klausberger, T. & Somogyi, P. Neuronal diversity and temporal dynamics: the unity of hippocampal circuit operations. *Science* **321**, 53–57 (2008).
72. O'Rourke, N.A., Weiler, N.C., Micheva, K.D. & Smith, S.J. Deep molecular diversity of mammalian synapses: why it matters and how to measure it. *Nat. Rev. Neurosci.* **13**, 365–379 (2012).
73. DeFelipe, J. *et al.* New insights into the classification and nomenclature of cortical GABAergic interneurons. *Nat. Rev. Neurosci.* **14**, 202–216 (2013).
74. Emes, R.D. & Grant, S.G. Evolution of synapse complexity and diversity. *Annu. Rev. Neurosci.* **35**, 111–131 (2012).
75. Micheva, K.D., Busse, B., Weiler, N.C., O'Rourke, N. & Smith, S.J. Single-synapse analysis of a diverse synapse population: proteomic imaging methods and markers. *Neuron* **68**, 639–653 (2010).
76. Micheva, K.D. & Smith, S.J. Array tomography: a new tool for imaging the molecular architecture and ultrastructure of neural circuits. *Neuron* **55**, 25–36 (2007).
77. Tsai, P.S. *et al.* Correlations of neuronal and microvascular densities in murine cortex revealed by direct counting and colocalization of nuclei and vessels. *J. Neurosci.* **29**, 14553–14570 (2009).
78. Oberlaender, M. *et al.* Cell type-specific three-dimensional structure of thalamocortical circuits in a column of rat vibrissal cortex. *Cereb. Cortex* **22**, 2375–2391 (2012).
79. Meyer, H.S. *et al.* Inhibitory interneurons in a cortical column form hot zones of inhibition in layers 2 and 5A. *Proc. Natl. Acad. Sci. USA* **108**, 16807–16812 (2011).
80. Meyer, H.S. *et al.* Number and laminar distribution of neurons in a thalamocortical projection column of rat vibrissal cortex. *Cereb. Cortex* **20**, 2277–2286 (2010).
81. Ascoli, G.A. *et al.* Petilla terminology: nomenclature of features of GABAergic interneurons of the cerebral cortex. *Nat. Rev. Neurosci.* **9**, 557–568 (2008).
82. Margrie, T.W. *et al.* Targeted whole-cell recordings in the mammalian brain *in vivo*. *Neuron* **39**, 911–918 (2003).
83. Kitamura, K., Judkewitz, B., Kano, M., Denk, W. & Hausser, M. Targeted patch-clamp recordings and single-cell electroporation of unlabeled neurons *in vivo*. *Nat. Methods* **5**, 61–67 (2008).
84. Angelo, K. *et al.* A biophysical signature of network affiliation and sensory processing in mitral cells. *Nature* **488**, 375–378 (2012).
85. Reid, R.C. From functional architecture to functional connectomics. *Neuron* **75**, 209–217 (2012).
86. Briggman, K.L., Helmstaedter, M. & Denk, W. Wiring specificity in the direction-selectivity circuit of the retina. *Nature* **471**, 183–188 (2011).
87. Bock, D.D. *et al.* Network anatomy and *in vivo* physiology of visual cortical neurons. *Nature* **471**, 177–182 (2011).
88. Wallace, D.J. *et al.* Single-spike detection *in vitro* and *in vivo* with a genetic Ca^{2+} sensor. *Nat. Methods* **5**, 797–804 (2008).
89. Akerboom, J. *et al.* Optimization of a GCaMP calcium indicator for neural activity imaging. *J. Neurosci.* **32**, 13819–13840 (2012).
90. Mank, M. *et al.* A genetically encoded calcium indicator for chronic *in vivo* two-photon imaging. *Nat. Methods* **5**, 805–811 (2008).
91. Ko, H. *et al.* Functional specificity of local synaptic connections in neocortical networks. *Nature* **473**, 87–91 (2011).
92. Holmgren, C., Harkany, T., Svennenfors, B. & Zilberter, Y. Pyramidal cell communication within local networks in layer 2/3 of rat neocortex. *J. Physiol.* **551**, 139–153 (2003).
93. Thomson, A.M., West, D.C., Wang, Y. & Bannister, A.P. Synaptic connections and small circuits involving excitatory and inhibitory neurons in layers 2–5 of adult rat and cat neocortex: triple intracellular recordings and biocytin labelling *in vitro*. *Cereb. Cortex* **12**, 936–953 (2002).
94. Song, S., Sjostrom, P.J., Reigl, M., Nelson, S. & Chklovskii, D.B. Highly nonrandom features of synaptic connectivity in local cortical circuits. *PLoS Biol.* **3**, e68 (2005).
95. Harvey, C.D., Collman, F., Dombeck, D.A. & Tank, D.W. Intracellular dynamics of hippocampal place cells during virtual navigation. *Nature* **461**, 941–946 (2009).
This study introduced the method of physiological recording in head-restrained mice on a spherical treadmill while the mice performed spatial tasks in a virtual environment.
96. Harvey, C.D., Coen, P. & Tank, D.W. Choice-specific sequences in parietal cortex during a virtual-navigation decision task. *Nature* **484**, 62–68 (2012).
97. Huber, D. *et al.* Multiple dynamic representations in the motor cortex during sensorimotor learning. *Nature* **484**, 473–478 (2012).
98. Fenno, L., Yizhar, O. & Deisseroth, K. The development and application of optogenetics. *Annu. Rev. Neurosci.* **34**, 389–412 (2011).
99. Koch, C. & Reid, R.C. Neuroscience: observatories of the mind. *Nature* **483**, 397–398 (2012).
100. Alivisatos, A.P. *et al.* Neuroscience. The brain activity map. *Science* **339**, 1284–1285 (2013).
101. Ahrens, M.B., Orger, M.B., Robson, D.N., Li, J.M. & Keller, P.J. Whole-brain functional imaging at cellular resolution using light-sheet microscopy. *Nat. Methods* **10**, 413–420 (2013).
102. Ahrens, M.B. *et al.* Brain-wide neuronal dynamics during motor adaptation in zebrafish. *Nature* **485**, 471–477 (2012).
103. Herrera, D.G. & Robertson, H.A. Activation of c-fos in the brain. *Prog. Neurobiol.* **50**, 83–107 (1996).
104. Barth, A.L., Gerkin, R.C. & Dean, K.L. Alteration of neuronal firing properties after *in vivo* experience in a FosGFP transgenic mouse. *J. Neurosci.* **24**, 6466–6475 (2004).
105. Grinevich, V. *et al.* Fluorescent Arc/Arg3.1 indicator mice: a versatile tool to study brain activity changes *in vitro* and *in vivo*. *J. Neurosci. Methods* **184**, 25–36 (2009).
106. Reijmers, L.G., Perkins, B.L., Matsuo, N. & Mayford, M. Localization of a stable neural correlate of associative memory. *Science* **317**, 1230–1233 (2007).